

Electronic Supplementary Information (ESI)

Effect of oxygen adsorption on the electrochemical oxidative corrosion of single-walled carbon nanotubes

Masato Tominaga,^{*a,b} Yuto Yatsugi^a and Makoto Togami^a

^[1] Graduate School of Science and Technology, Kumamoto University, Kumamoto 860-8555, Japan.

^[2] Kumamoto Institute for Photo-Electro Organics (Phoenics), Kumamoto 862-0901, Japan.

Corresponding author

Masato Tominaga

Graduate School of Science and Technology, Kumamoto University, Kumamoto 860-8555, Japan.

E-mail: masato@gpo.kumamoto-u.ac.jp

Tel/Fax: +81-96-342-3655

Experimental Section

Synthesis and characterization of single-walled carbon nanotubes (SWCNTs)

SWCNTs were synthesized on a gold wire surface by chemical vapor deposition, as described previously.¹⁻³ The gold wire surface was completely covered with SWCNTs, as determined by its absence of any electrochemical behavior characteristic of gold at any current.

Field-emission scanning electron microscopy indicated SWCNT bundles of 5–20 nm in diameter. The thickness of the SWCNT layer was *ca.* 20 μm . Transmission electron microscopy images indicated individual tubular structures. The wall thickness was *ca.* 0.35 nm (Fig. S1), indicating that they were SWCNTs.⁴⁻⁸

The prominent feature of the Raman spectra of SWCNTs is the *G*-band at *ca.* 1,590 cm^{-1} .^{9,10} The *G*-band is a doubly-degenerate phonon Raman active mode for sp^2 -hybridized carbon networks. The other feature is the *D*-band at *ca.* 1,350 cm^{-1} . This is localized at imperfect lattice structure regions, particularly the edges and defects of sp^2 -hybridized structures.^{9,10} The *G*-band/*D*-band intensity ratio (I_G/I_D) was used to evaluate the crystallinity of the sp^2 -hybridized structure. The I_G/I_D ratio of the SWCNTs was *ca.* 35, when a 514.5 nm laser excitation source was used. The *D*-band was very weak, indicating that the SWCNTs were of high crystallinity and had few defects. The radial breathing mode of the SWCNTs gives information about the diameter distribution of the SWCNTs. The SWCNTs has a diameter distribution of 0.9–1.6 nm, as estimated from:

$$d/\text{nm} = 248/(\nu/\text{cm}^{-1}), \quad (1)$$

where d is the SWCNT diameter and ν is the Raman shift.¹¹⁻¹³

Estimation of adsorbed oxygen on the SWCNTs and highly oriented pyrolytic graphite (HOPG)

The charge flow was estimated to be 8.4×10^{-5} C, based on the area of the oxygen reduction current in the first voltammogram scan of the SWCNTs in Fig. 1a. Thus, the adsorbed oxygen content was 2.2×10^{-10} mol, assuming the oxygen reduction current represented a four-electron reduction. The specific surface area of the SWCNTs as determined by Brunauer–Emmett–Teller

analysis was $9 \times 10^2 \text{ cm}^2$. A single benzene (area of one side: $7.09 \times 10^{16} \text{ cm}^2$) unit 1.4×10^{15} pieces cm^{-2} . Thus, the SWCNT surface area of $9 \times 10^2 \text{ cm}^2$ constituted 1.26×10^{18} benzene units. From this information, the amount of oxygen adsorbed at the SWCNTs was estimated to be 5.2×10^{-5} per carbon atom.

Similarly, the amount of oxygen adsorbed at HOPG was estimated to be 3.0×10^{-4} per carbon atom. This was higher than expected, probably because of surface defects formed during the peeling process used to prepare the fresh surface. This prediction was supported by the calculated surface specific capacitance per geometric area of $50 \mu\text{F cm}^{-2}$, which was nearly 15 times larger than that previously reported ($2\text{--}3 \mu\text{F cm}^{-2}$).¹⁴

Assignment of Raman peaks of β -carotene

The ν_1 , ν_2 , ν_3 and ν_4 peaks at 1,541, 1,157, 1,007 and 945 cm^{-1} were assigned to the conjugated C=C stretching, C=C+C-C stretching and C-H bending, C-CH₃ stretching (main-chain C-CH₃ side group), and out-of-plane C-H wagging modes, respectively.¹⁵⁻¹⁷

References

- [1] M. Tominaga, S. Sakamoto and H. Yamaguchi, *J. Phys. Chem. C*, 2012, **116**, 9498.
- [2] M. Tominaga, M. Togami, M. Tsushida and D. Kawai, *Anal. Chem.*, 2014, **86**, 5053.
- [3] S. Sakamoto and M. Tominaga, *Chem. Asian J.*, 2013, **8**, 2680.
- [4] Iijima, S. *Nature* 1991, **354**, 56.
- [5] A. K. Geim and K. S. Novoselov, *Nature Mater.* 2007, **6**, 183.
- [6] P. R. Wallace, *Phys. Rev.* 1947, **71**, 622.
- [7] R. Saito, G. Dresselhaus and M. S. Dresselhaus, *Physical Properties of Carbon Nanotubes*; Imperial College Press: London, 1998.
- [8] R. L. McCreery, *Chem. Rev.* 2008, **108**, 2646.
- [9] F. Tuinstra and J. L. J. Koenig, *Chem. Phys.* 1970, **53**, 1126.
- [10] F. Tuinstra and J. L. J. Koenig, *Composite. Mater.* 1970, **4**, 492.
- [11] R. Saito, G. Dresselhaus and M. S. Dresselhaus, *Phys. Rev. B* 2000, **61**, 2981.

- [12] A. Jorio, R. Saito, J. H. Hafner, C. M. Lieber, M. Hunter, T. McClure, G. Dresselhaus and M. S. Dresselhaus, *Phys. Rev. Lett.* 2001, **86**, 1118.
- [13] H. Kataura, Y. Kumazawa, Y. Maniwa, I. Umezu, S. Suzuki, Y. Ohtsuka and Y. Achiba, *Synth. Met.* 1999, **103**, 2555.
- [14] R. J. Rice and R. L. McCreery, *Anal. Chem.*, 1989, **61**, 1637.
- [15] K. Yanagi, Y. Miyata and H. Kataura, *Adv. Mater.*, 2006, **18**, 437.
- [16] P. Horn and M. Kertesz, *J. Phys. Chem. C*, 2010, **114**, 12139.
- [17] K. Yanagi, K. Iakoubovskii, S. Kazaoui, N. Minami, Y. Maniwa, Y. Miyata and H. Kataura, *Phys. Rev. B*, 2006, **74**, 155420.

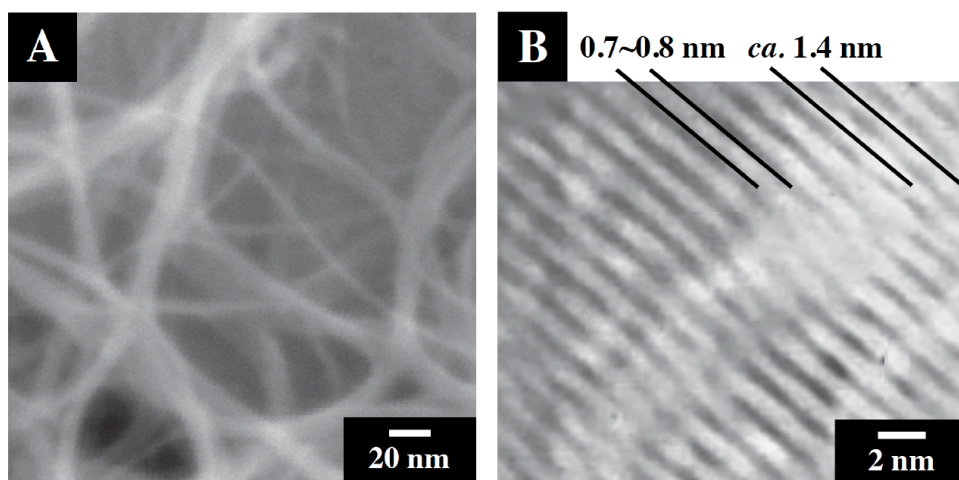


Fig. S1 (a) Transmission electron microscopic and (b) high-resolution transmission electron microscopic images of the single-walled carbon nanotubes.